
RealCraft: Attention Control as A Tool for Zero-Shot Consistent Video Editing

Shutong Jin
KTH

shutong@kth.se

Ruiyu Wang
KTH

ruiyuw@kth.se

Florian T. Pokorny
KTH

fpokorny@kth.se

Abstract

Even though large-scale text-to-image generative models show promising performance in synthesizing high-quality images, applying these models directly to image editing remains a significant challenge. This challenge is further amplified in video editing due to the additional dimension of time. This is especially the case for editing real-world videos as it necessitates maintaining a stable structural layout across frames while executing localized edits without disrupting the existing content. In this paper, we propose *RealCraft*, an attention-control-based method for zero-shot real-world video editing. By swapping cross-attention for new feature injection and relaxing spatial-temporal attention of the editing object, we achieve localized shape-wise edit along with enhanced temporal consistency. Our model directly uses Stable Diffusion and operates without the need for additional information. We showcase the proposed zero-shot attention-control-based method across a range of videos, demonstrating shape-wise, time-consistent and parameter-free editing in videos of up to 64 frames.

1 Introduction

Recent advancements in large-scale text-driven diffusion models such as DALL-E 3 Betker et al. [2023], Imagen Saharia et al. [2022], Stable Diffusion Rombach et al. [2022b], and SORA Brooks et al. [2024] have shown remarkable capabilities in generating high-quality and diverse visual content with only textual inputs. However, there is no smooth transfer from visual generation to text-driven editing, since diffusion models only know what to change but not what to preserve with given text prompts Parmar et al. [2023]. Additionally, compared with synthetic data, semantic editing of real-world images or videos poses extra challenges in maintaining structural consistency and preserving localization. This is due to the fact that, for synthetic editing, the original images or videos are typically sampled from the latent space of diffusion models, based on source textual prompts Hertz et al. [2022]. Semantic information of visual content is therefore well preserved during the sampling process. Real-world images and videos on the other hand feature cluttered scenes, occluded objects or moving camera views Bar-Tal et al. [2022] whose semantic information may not be fully captured by diffusion models. Furthermore, for video editing, there is a trade-off between maintaining temporal consistency and enforcing localized and significant changes Lee et al. [2023]. Thus, most editing of real-world videos to date is still limited to style transfer Yang et al. [2023]. For simplicity, we refer to real-world videos (as opposed to synthetically generated videos) as real videos in the following paper.

Existing methods for text-driven real video editing often deploy image diffusion models, e.g., Stable Diffusion, for frame-wise edits while utilizing deterministic DDIM Song et al. [2020] for image-to-noise inversion. Three major methods are used to maintain the original layouts of the frames. One is to impose structural information such as Canny edges, human poses and bounding boxes utilizing ControlNet Zhang et al. [2023], thereby guiding the frame sampling process Zhao et al. [2023a], Jeong and Ye [2023]. Another stream of work provides structural editing information

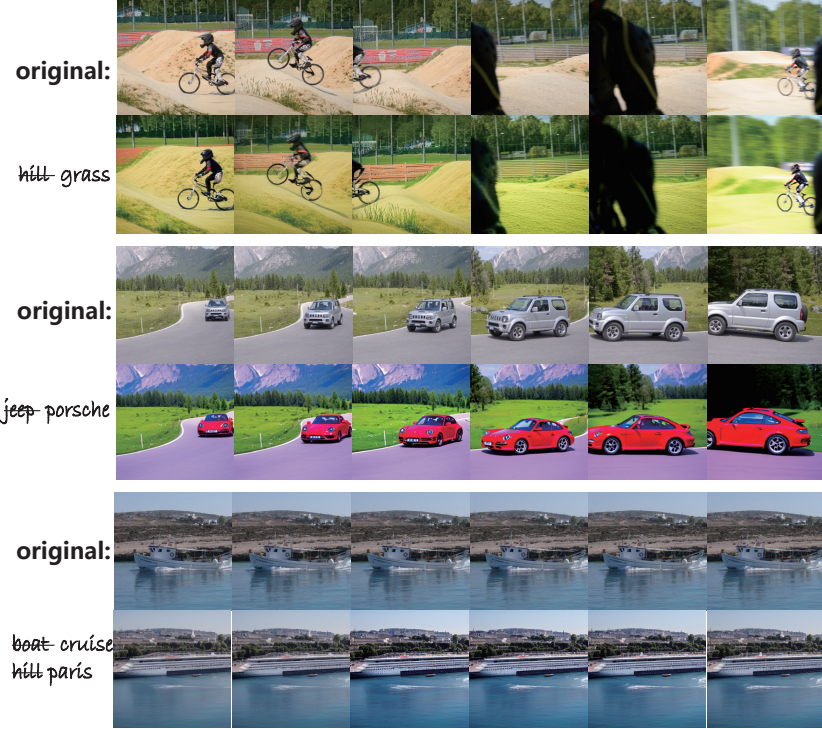


Figure 1: *RealCraft* enables zero-shot, shape-wise, consistent editing for real videos. Our method performs edits using Stable Diffusion, with text as the only input. No extra training or fine-tuning of models, structural guidance or parameter tuning is required.

through Atlas layer Bar-Tal et al. [2022], Couaron et al. [2023], Chai et al. [2023], Lee et al. [2023] and various reference-frame-based methods Yan et al. [2023], Geyer et al. [2023] are also deployed to maintain temporal consistency. In the aforementioned methods, additional inputs describing the structural information or supplementary models for generating intermediate data are usually needed and typically lack precise control over localized information, leading to challenges in compositional consistency He et al. [2023]. Attention-control-based methods inject new editing features during the denoising process by deploying the semantic relations in the cross-attention Hertz et al. [2022] or self-attention Ceylan et al. [2023], Wu et al. [2023] maps generated by pre-trained diffusion models. Using these approaches, zero-shot text-driven video editing is achieved Qi et al. [2023]. However, these methods typically lack significant edits, e.g. shape and texture, over original frames or require precise tuning of parameters.

In this paper, we propose *RealCraft*, a zero-shot method for text-driven shape-wise real video editing requiring no extra parameters. Our proposed method controls the attention maps generated by Stable Diffusion Rombach et al. [2022b] and achieves a balance between significant localized edits and temporal consistency in edited videos. The method is built upon two key observations: i) An entire injection of cross-attention may cause instability across frames in real video editing. ii) Although spatial-temporal attention contributes to overall consistency, it overshadows new features injected by cross-attention. Based on the two observations, we design a two-step attention-control approach. Firstly, we propose to directly swap the cross-attention maps of the editing objects and inject the features during all DDIM denoising timesteps, thereby stabilizing the structure while localizing the edits. At the same time, we propose to relax the spatial-temporal attention’s influence on new feature injection by masking out the feature-heavy areas, enabling significant shape edits while ensuring temporal consistency.

This two-step approach opens up the possibility for significant and consistent shape edits via swapping cross-attention for new feature injection and relaxing spatial-temporal attention for enhanced temporal consistency. This addresses a longstanding challenge in zero-shot real video editing, where normally a choice has to be made between these two aspects. The efficacy of the proposed method also alleviates

attention-based methods’ burden of careful parameter tuning, e.g., blending threshold, blending steps. The main contributions of our work are as follows.

- We introduce *RealCraft*, an effective method for zero-shot real video editing, featuring in significant shape editing ability with enhanced temporal consistency.
- We provide two key observations behind attention mechanism and propose a two-step approach of swapping cross-attention and relaxing spatial-temporal attention.
- We propose a localized cross-attention swapping technique. Specifically, it maintains the original prompt’s cross-attention after swapping, thereby ensuring stable feature injection.
- Qualitative and quantitative experiments have been conducted across various baselines, showcasing the efficacy of the proposed method on consistent video editing, background transformation, shape-wise editing, and pose preservation.

2 Related Work

2.1 Diffusion Model for Text-driven Video Editing

Diffusion Models (DMs) Ho et al. [2020] feature a step-wise denoising process, which facilitates enhanced control over sampling. Therefore, in recent years, DMs are widely studied for text-to-image generation Betker et al. [2023], Saharia et al. [2022], Rombach et al. [2022b] and image editing Sheynin et al. [2023], Kawar et al. [2023], Parmar et al. [2023]. Text-driven video editing often takes advantages of the powerful pre-trained text-to-image models and adds effective control during the sampling process in preservation of structural layout and temporal consistency. ControlNet Zhang et al. [2023] for conditional control in pre-trained diffusion models is a widely adopted approach Ouyang et al. [2023], Liao and Deng [2023], Yang et al. [2023]. Diverse conditional controls are deployed, for example, HED boundaries Zhao et al. [2023a], various edge maps Feng et al. [2023], depth maps Yan et al. [2023], poses Zhao et al. [2023b] and bounding boxes Jeong and Ye [2023], catering to facial editing, structure maintenance, gesture preservation and target localization. However, this method requires choosing specified types of control for different video prompts and expertise in integration when multiple controls are needed.

Neural Atlases (NLA) model-based methods Kasten et al. [2021], Couairon et al. [2023], Lee et al. [2023], Huang et al. [2023] are popular for their capacity to decompose inputs into layered representations, such as foreground and background atlases, ensuring scene consistency. Notable examples include Text2Live Bar-Tal et al. [2022], which introduces additional edit layers to atlases and trains a specific generator for these layers. StableVideo Chai et al. [2023] enhances temporal consistency with an atlas aggregation network. However, the diversity of these methods is constrained by the object layer setup, or they require different pre-trained models for various videos.

Other methods include FuseYourLatent Lu et al. [2023], which fuses latents directly during editing, and TokenFlow Geyer et al. [2023], which propagates diffusion features using inter-frame correspondences. Dreamix Molad et al. [2023], on the other hand, corrupts the original video via down-sampling and focuses on fine-tuning for motion consistency, often at the expense of structural consistency.

2.2 Attention Control for Image and Video Editing

In addition to the aforementioned methods, attention-control-based approaches are becoming increasingly popular because they typically do not require additional input beyond text prompt and input video. Attention control for text-driven image and video editing generally involves two categories: self-attention control and cross-attention control. Since cross-attention can bridge between semantic information and image spatial layout, it has been widely adopted in image editing works Wang et al. [2023a], Chen et al. [2023], Choi et al. [2023], Park et al. [2023]. For instance, Prompt-to-Prompt Hertz et al. [2022] realizes localized image editing by replacing, refining, or reweighing the prompts’ cross-attention weights. pix2pix-zero Parmar et al. [2023] achieves structurally coherent image editing by using cross-attention as guidance.

When extending the editing target to videos, both self-attention and cross-attention can be effectively utilized to incorporate features from the target prompt while ensuring temporal consistency.

Addressing the common flickering issue, Tune-A-Video Wu et al. [2023] introduced sparse-casual spatial-temporal attention to guarantee consistent generation. FateZero Qi et al. [2023] leverages the cross-attention of moving objects to mask spatial-temporal attention through a user-specified blending threshold, minimizing background changes during feature injection. Video-P2P Liu et al. [2023] adapts the cross-attention control from Prompt-to-prompt, initially used in image editing, to video editing by integrating sparse-causal attention in the temporal domain. LOVECon Liao and Deng [2023] processes the source video by dividing it into consecutive windows, sequentially editing the frames while using cross-attention across these windows to maintain temporal consistency. However, maintaining strong temporal consistency often limits the freedom to introduce significant edits and thus restricts edits mainly to style transfer. While editing object shape by masking self-attention can potentially lead to instability if the blending threshold is not appropriately chosen. In this paper, we address these challenges by swapping cross-attention and relaxing spatial-temporal attention, allowing consistent shape-wise editing.

3 Methodology

3.1 Preliminary

Latent Diffusion Models. Denoising Diffusion Probabilistic Models (DDPMs) Ho et al. [2020] are generative models that capture a data distribution $q(x)$ with a U-Net Ronneberger et al. [2015] ϵ_θ . Latent Diffusion Models (LDMs) Rombach et al. [2022b] are variants of DDPMs in which the diffusing and denoising process are operated in the latent space of an autoencoder. An encoder \mathcal{E} reduces an RGB image x to a low-dimensional latent variable $z = \mathcal{E}(x)$, which is then approximated back to pixel space by decoder \mathcal{D} as $\mathcal{D}(z) \approx x$. Text inputs can be incorporated into the model as guidance allowing semantic modifications of the input images. The objective of LDMs and text-driven LDMs is to minimize the losses, as shown in *Eq. 1* and *Eq. 2*.

$$\mathcal{L}(\theta) = \mathbb{E}_{z_0 \sim q(\mathcal{E}(x_0)), \epsilon \sim \mathcal{N}(0, I), t} \|\epsilon - \epsilon_\theta(z_t, t)\|_2^2, \quad (1)$$

$$\mathcal{L}_p(\theta) = \mathbb{E}_{z_0 \sim q(\mathcal{E}(x_0)), \epsilon \sim \mathcal{N}(0, I), t} \|\epsilon - \epsilon_\theta(z_t, t, p)\|_2^2, \quad (2)$$

where $p = \psi(P)$ is the embedding of the conditional text prompt P and z_t is a noisy sample of z_0 at timestep t , ϵ is a random Gaussian noise.

DDIM Inversion and Sampling. Denoising diffusion implicit model (DDIMs) Song et al. [2020] are special cases of DDPMs where the sampling process is deterministic, and are thus employed for the inversion process for image and video editing tasks. The deterministic property not only accelerates the sampling process, but enables semantic interpolation in the latent variables whose consistency are ensured by deterministic sampling.

Random noise z_T is converted to a clean latent z_0 in a sequence of timestep $t : T \rightarrow 1$:

$$z_{t-1} = \sqrt{\alpha_{t-1}} \frac{z_t - \sqrt{1 - \alpha_t} \epsilon_\theta}{\sqrt{\alpha_t}} + \sqrt{1 - \alpha_{t-1}} \epsilon_\theta, \quad (3)$$

Grounded in the ODE limit analysis of the diffusion process, the DDIM inversion method is designed to transform a clean latent \hat{z}_0 into its corresponding noised version \hat{z}_T through a reverse sequence of steps $t : 1 \rightarrow T$:

$$\hat{z}_t = \sqrt{\alpha_t} \frac{\hat{z}_{t-1} - \sqrt{1 - \alpha_{t-1}} \epsilon_\theta}{\sqrt{\alpha_{t-1}}} + \sqrt{1 - \alpha_t} \epsilon_\theta. \quad (4)$$

where α_t is the parameter for noise scheduling.

Eq. 4 is employed to reverse the clean latent of the original video into its noised counterpart, followed by the application of *Eq. 3* to sample the edited video from this noise space.

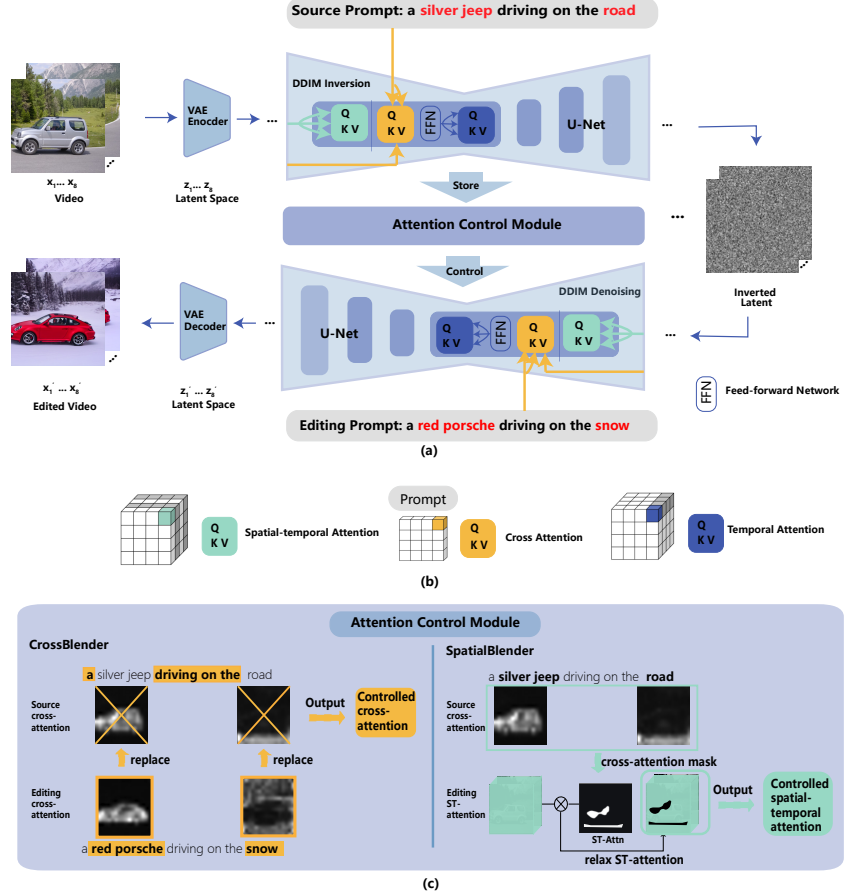


Figure 2: (a) Our proposed *RealCraft* pipeline takes source frames $\{x_i\}_{i=1}^n$ ($n = 8$ in this illustration), source prompt, and editing prompt as inputs. Initially, $\{x_i\}_{i=1}^n$ are encoded into latent space by a VAE Kingma and Welling [2013] encoder, followed by DDIM inversion to obtain the inverted latents, while storing spatial-temporal and cross-attention maps. In the denoising stage, the stored attention maps are fed into the Attention Control Module, orchestrating the spatial-temporal (SPATIALBLENDER) and cross-attention (CROSSBLENDER) for video editing. (b) Illustrations of spatial-temporal attention, cross attention, and temporal attention, with different colors representing the QKV components. Cross-attention occurs between the encoded prompt and frame. (b) The proposed Attention Control Module comprises CROSSBLENDER and SPATIALBLENDER.

3.2 Attentions within *RealCraft*

In Stable Diffusion Rombach et al. [2022b], a U-Net architecture comprising 2D blocks with spatial self-attention and cross-attention layers is employed during DDIM inversion and denoising process for text-to-image generation. Specifically, cross-attention aligns the image spatial layout with a text prompt, while self-attention provides consistency within the image. In *RealCraft*, we utilize cross-attention between embedded frames $[z_t]_{t=1}^T$ and encoded editing prompts p to inject editing features and follow the design of Tune-A-Video Wu et al. [2023] to inflate 2D self-attention into 3D spatial-temporal attention, enabling video editing. $\text{CROSS-ATTN}(Q_c, K_c, V_c)$ and $\text{ST-ATTN}(Q_{st}, K_{st}, V_{st})$ are defined as follows.

$$Q_c = W^{Q_c} \cdot z_t^k, K_c = W^{K_c} \cdot p, V_c = W^{V_c} \cdot p \quad (5)$$

$$Q_{st} = W^{Q_{st}} \cdot z_t^k, K_{st} = W^{K_{st}} \cdot [z_t^1, z_t^{k-1}], V_{st} = W^{V_{st}} \cdot [z_t^1, z_t^{k-1}] \quad (6)$$

where the $k \in [1, K]$, K is the number of total frames to edit, z_t^k represent the frame k in latent space at timestep t ; $W^{Q_c}, W^{K_c}, W^{V_c}, W^{Q_{st}}, W^{K_{st}}, W^{V_{st}}$ are projection matrices from the pre-trained model Rombach et al. [2022b]. An illustration of types of Attention used are shown in *Fig. 2 (b)*.

As illustrated in *Fig. 2*, during the inversion process, all blocks of cross-attention maps for each word within the source prompt and spatial-temporal attention maps are stored. This storing concept was introduced by FateZero Qi et al. [2023] to enable zero-shot editing. We use the stored source attention maps to facilitate cross-attention swapping and spatial-temporal attention relaxing for consistent new feature injection during the denoising stage with the proposed Attention Control Module.

Some notations are introduced for clarity: $P^{src} = \{p_i^{src} \mid i \in [1, M]\}$, $P^{edit} = \{p_i^{edit} \mid i \in [1, M]\}$ denote the source and editing prompts, M is the total number of words in the prompt. $W^{src} = \{w_j^{src} \mid j \in [1, N]\}$, $W^{edit} = \{w_j^{edit} \mid j \in [1, N]\}$ represent the words to be modified in P^{src} and the replacement words in P^{edit} , where N is the number of words to edit. At timestep t during denoising, the cross-attention maps $c_{i,t}^{edit} \in C_t^{edit}$ for each element in P^{edit} and the spatial-temporal attention map s_t^{edit} are calculated. Correspondingly, the stored cross and spatio-temporal attention maps of source prompts during the inversion are $[C_t^{src}]_{t=1}^T = \{c_{i,t}^{src} \mid i \in [1, M]\}$ and $[s_t^{src}]_{t=1}^T$.

3.3 Attention Control Module in *RealCraft*

The Attention Control Module comprises two key components: CROSSBLENDER and SPATIALBLENDER, tasked with swapping cross-attention and relaxing spatial-temporal attention, respectively.

3.3.1 CrossBlender

Prompt-to-prompt Hertz et al. [2022] introduces cross-attention maps for feature injection in text-driven image editing. Specifically, the entire source prompt’s cross-attention maps are injected during the DDIM denoising, and an injection interval needs to be decided. We observe that this step-function-like injection does not accommodate video editing’s consistency requirement, as structural instability can be introduced when edits are not localized, examples can be found in *Fig. 5*. Our CROSSBLENDER adopts a distinct approach in swapping the cross-attention maps: i) Rather than directly injecting the entire source prompt maps, we swap the cross-attention map of the editing target (from W^{src} to W^{edit}), which implies the cross-attention injected during the denoising is a combination of source maps $[C_t^{src}]_{t=1}^T$ stored during the DDIM inversion process and new maps calculated by *Eq. 5* for W^{edit} . This localizes changes by swapping specific words, resulting in new feature injection along with minimal influence on the structural layout of each frame. ii) Instead of injecting new features from certain timestep, our CROSSBLENDER outputs the swapped cross-attention maps during the whole denoising process. This complete injection provides a stable source of new features and alleviates the need to choose a specific injecting interval. The mathematical representation of CROSSBLENDER at timestep t is as follows.

$$\text{CROSSBLENDER}(C_t^{src}, C_t^{edit}) = \{c_{i,t}\}_{i=1}^M = \begin{cases} c_{i,t}^{src} & \text{for } p_i^{edit} \text{ not in } W^{edit} \\ c_{i,t}^{edit} & \text{for } p_i^{edit} \text{ in } W^{edit} \end{cases} \quad (7)$$

3.3.2 SpatialBlender

Another key observation from us is that spatial-temporal attention, although contributes to overall temporal consistency, can largely weaken the injection of new features through cross-attention. As a result, the edited frames often closely resemble the source frames in shape, color and texture, making the modifications on objects and background less noticeable, examples can be found in *Fig. 4* and *Fig. 5*. This is partially because the DDIM inversion process involves a trade-off between distortion and editability Tov et al. [2021], where enhancing reconstruction by reducing prompt influence limits the capacity for significant edits Hertz et al. [2022]. We find that by relaxing the spatial-temporal attention in the feature-heavy area, significant shape edits with enhanced temporal consistency can be made.

Relaxation here refers to masking out feature-heavy areas in the original spatial-temporal attention s_t^{src} , and replacing the rest with the editing spatial-temporal attention s_t^{edit} . The feature-heavy area can be extracted from a blending mask M_t , generated with *Eq. 8* using stored cross-attention maps C_t^{src} with fixed τ equals to 0.5. Conversely, FateZero Qi et al. [2023] proposes to mask out the edited area to keep the original structure unchanged, with the same *Eq. 8* but user-specified τ . However, as shown in *Fig. 3*, the shape of M_t varies a lot with different τ . This could be why FateZero’s performance is highly dependent on the careful selection of the threshold value to prevent flickering issues. This is

due to the fact that, even though spatial-temporal attention limits significant edits, it still contributes to the overall consistency. Thus when relaxing the spatial-temporal attention, a higher consistency requirement for the features injected by cross-attention is raised. And CROSSBLENDER is able to provide a more stable source of features rather than solely relying on the cross-attention between inverted latent and the editing prompt. The mathematical representation of SPATIALBLENDER at timestep t is as follows.

$$M_t = \text{STEP}(C_t^{\text{src}}, 0.5) \quad (8)$$

$$\text{SPATIALBLENDER}(C_t^{\text{src}}, s_t^{\text{src}}, s_t^{\text{edit}}) = M_t \odot s_t^{\text{edit}} + (1 - M_t) \odot s_t^{\text{src}} \quad (9)$$

where STEP is a Heaviside step function with a constant threshold equals to 0.5. Note that spatial blending only works for editing words W^{edit} .

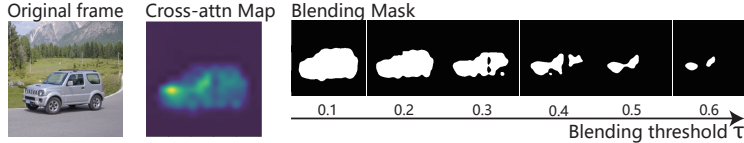


Figure 3: A demonstration of the impact of blending threshold τ on blending mask.

3.3.3 Algorithm

The general algorithm of *RealCraft* video editing with CROSSBLENDER and SPATIALBLENDER is shown in *Algorithm 1*.

Algorithm 1 *RealCraft* video editing

```

1: Input: original video  $X$ , source prompt  $P^{\text{src}}$ , editing prompt  $P^{\text{edit}}$ 
2: Output: Edited video  $X^{\text{edit}}$ 
3:  $z_0 \leftarrow \mathcal{E}(X)$ ;
4:  $z_T, [C^{\text{src}}]_{t=1}^T, [s^{\text{src}}]_{t=1}^T = \text{DDIM\_INV}(z_0, P^{\text{src}})$ ;
5:  $z_T^* \leftarrow z_T$ ;
6: for  $t = T; T - 1, \dots, 1$  do
7:    $z_{t-1}, C_{t-1}^{\text{edit}}, s_{t-1}^{\text{edit}} \leftarrow \text{DDIM}(z_t, P^{\text{edit}}, t)$ ;
8:    $C_{t-1}^{\text{edit}*} \leftarrow \text{CROSSBLENDER}(C_{t-1}^{\text{src}}, C_{t-1}^{\text{edit}})$ ;
9:    $s_{t-1}^{\text{edit}*} \leftarrow \text{SPATIALBLENDER}(C_{t-1}^{\text{src}}, s_{t-1}^{\text{src}}, s_{t-1}^{\text{edit}})$ ;
10:   $z_{t-1}^* \leftarrow \text{DDIM}(z_t^*, P^{\text{edit}}, t) \{ C_{t-1}^{\text{edit}} \leftarrow C_{t-1}^{\text{edit}*}, s_{t-1}^{\text{edit}} \leftarrow s_{t-1}^{\text{edit}*} \}$ ;
11: end for
12:  $X^{\text{edit}} \leftarrow \mathcal{D}(z_0^*)$ 
13: return  $X^{\text{edit}}$ 

```

4 Experiments

4.1 Implementation Details

For most of the editing tasks, we directly employ *stable-diffusion-v1-4* Rombach et al. [2022a] as the pre-trained model with a total DDIM timestep of $T = 30$. In the quantitative evaluation, to ensure fair evaluation and accommodate baselines requiring atlas layers, whose extraction requires training of models for each video, we utilize the dataset in NLA Kasten et al. [2021], sourced from the DAVIS dataset Pont-Tuset et al. [2017], comprising real videos ranging from 43 to 70 frames. These frames are further segmented into non-overlapping sets of eight consecutive frames, each paired with 2 or 3 editing prompts, to conduct the evaluation. Across all baselines, where applicable, a uniform blending threshold of 0.5, fixed blending steps $t \in [0.5T, T]$, pre-trained atlas layer sourcing from NLA Kasten et al. [2021] are adopted to ensure fair evaluation.

4.2 Metrics

Our user study evaluated the editing quality, editing consistency, and edited video fidelity across 64 videos with 29 subjects. The subjects were presented with the original video and 7 anonymous

edited videos at the same time, then asked to grade each video on a scale from 1 (Very bad) to 5 (Very good). Additionally, we use the same quantitative metrics adopted by the FateZeroQi et al. [2023], the metrics are as follows:

- **Tem-Con Esser et al. [2023].** This metric assesses temporal consistency in video frames by calculating the cosine similarity across all pairs of consecutive frames.
- **Frame-Acc Parmar et al. [2023].** This refers to frame-wise editing accuracy, quantified as the proportion of frames where the edited image exhibits higher CLIP similarity Radford et al. [2021] to the editing prompt compared to the source prompt.
- **Edit (User Study).** This evaluates the quality of edits, focusing on how well they align with the prompt, and the suitability of shape, background, and object features.
- **Temp (User Study).** Edited video’s temporal consistency and its adherence to the original video’s sequence.
- **Fidelity (User Study).** Average score representing participants’ perceived video fidelity ranging from artificial (1) to real (5).

4.3 Baseline Comparisons

Quantitative evaluations of our proposed method in comparison with state-of-the-art zero-shot video editing baselines are performed. We select 6 baselines, each as a representative of one category within the spectrum of video editing methodologies, covering three mainstream approaches outlined in Section 2: attention-control-based, ControlNet, and NLA-based methods. i) FateZero Qi et al. [2023] conducts editing through masking the spatial-temporal attention with binary cross-attention masks. ii) Tune-A-Video Wu et al. [2023] generates similar content by overfitting an inflated diffusion model on a single video. iii) TokenFlow Geyer et al. [2023] leverages the original inter-frame feature correspondences when editing features to achieve better temporal consistency. iv) LOVECon Liao and Deng [2023] adopts ControlNet Zhang et al. [2023] to guide the denoising process, employing cross-attention across frames’ windows to facilitate long video editing. v) StableVideo Chai et al. [2023] performs consistent shape-aware video editing through updating the models Neural layered atlas (NLA) via editing key video frames and vi) Video-P2P Liu et al. [2023] expands Prompt-to-Prompt Hertz et al. [2022]’s cross-attention control from image to video editing by incorporating spatial-temporal attention.

Table 1: Quantitative evaluation against baselines on dataset provided in NLA Kasten et al. [2021].

Method	CLIP Metrics↑		User Study↑		
	Tem-Con	Frame-Acc	Edit	Temp	Fidelity
FateZero Qi et al. [2023]	0.9564	<u>0.9043</u>	2.26	2.11	2.41
Tune-A-Video Wu et al. [2023]	0.9718	0.8544	3.26	3.37	3.33
TokenFlow Geyer et al. [2023]	0.9303	0.7574	<u>3.41</u>	4.26	<u>3.81</u>
LOVECon Liao and Deng [2023]	0.8859	0.6545	1.89	1.01	1.44
StableVideo Chai et al. [2023]	0.9238	0.8469	1.67	3.00	1.78
Video-P2P Liu et al. [2023]	0.8798	0.8689	2.48	2.00	1.56
Ours - C. only	<u>0.9727</u>	0.8700	—	—	—
Ours - C. + S.	0.9774	0.9542	3.74	3.74	3.93

C. only stands for only *CrossBlender* is used.

C. + S. stands for both *CrossBlender* and *SpatialBlender* are used.

The highest performances are highlighted in bold, the second-best results are marked with an underline.

4.4 Experimental Results

Tab. 1 displays the performance of our method and various baselines. Our approach outperforms others in both metrics. “Tem-Con” measures the temporal consistency across edited frames while “Frame-Acc” evaluates the edited video’s alignment with the editing prompt, reflecting whether significant changes have been made in the edits. In our user study, our method was rated highest for edit quality and fidelity, and second for temporal consistency, with TokenFlow being the top in that category.

Fig. 4 - 5 display the qualitative comparison. In *Fig. 4*, significant background modifications are made to align with editing prompts, such as transforming forests into deserts or snowy landscapes, with *RealCraft* adding specific features like desert terrain and snow on trees, a feature rarely presented by the others.



Figure 4: Qualitative comparison with other baselines in background transformation.

Fig. 5 showcases the selected methods' proficiency in shape editing and pose preservation. Full frames and more examples can be found in the supplementary material. In (a), *RealCraft* and *Video-P2P* transform the boat into a kayak with significant shape changes. *FateZero* struggles in adding the new object, likely due to sensitivity in selecting the optimal blending threshold. Even though *Tune-A-Video*, *TokenFlow*, *LOVECon* and *StableVideo* convert the boat to a kayak, the shape of the kayak still follows the original structure of the boat, which results in reduced video fidelity. We observe similar results in (b), where some methods appear less effective in capturing a realistic shape and texture of the beret, with the color distribution remaining similar to the original helmet.

Fig. 5 (c) compares the models' ability in pose preservation, the information of which is not fully observable from frame and text. *FateZero*, *LOVECon* and *Video-P2P* fail to maintain the original pose and orientation of the lion. Furthermore, our method ensures higher editing fidelity as shown in (d). When transforming the black swan to flamingo, alternation of the neck curvature of the swan leads to enhanced fidelity, which is not conveyed in some methods. This serves as a supplementary example of a successful shape edit: the design of Attention Control Module appears to allow adequate new feature injection in this example.

It can be concluded that while the attention-controlled-based *FateZero*, *LOVECon* and *Video-P2P* succeed in introducing new features, flickering issues are often observed, likely due to the sensitivity of blending threshold and timesteps. Among them, *Video-P2P* also faces challenges in preserving the original structural layout across frames, suggesting more localized control instead of step-function-like swapping over cross-attention is needed for videos. *Tune-A-Video* and *TokenFlow* maintain strong temporal consistency, yet the edits often resemble the original frames in terms of color and shape. The NLA-based *StableVideo* demonstrates good performance in both shape editing and temporal consistency, however, the fidelity issues, potentially due to the layer-wise editing, are raised in the user study. Experimental results indicate that our method improves the editing performance by balancing significant edits and temporal consistency.

4.5 Applications

4.5.1 Consistent Video Editing.

RealCraft supports temporal-consistent video editing up to 64 frames using a sliding window approach. It processes 8 frames at a time without any overlap or prior information on previous frames. An example is shown in *Fig. 6*, where the original video features a small dog moving quickly under and with occlusions caused by leaves, poles, and fences. Our method transforms the dog into a cat while preserving the video's overall temporal consistency. Another example can be found in *Fig. 1* hill-to-grass, the edits remain stable with fast-moving objects and severe occlusions.

4.5.2 Background Transformation.

When performing the background transformation with attention-control-based methods, we observe that the edited background closely resembles the original one in terms of texture and color distribution. Leveraging the relaxation of spatial-temporal attention and the swapping of cross-attention, *RealCraft* neutralizes the influence of the original structure while introducing new features, preventing them

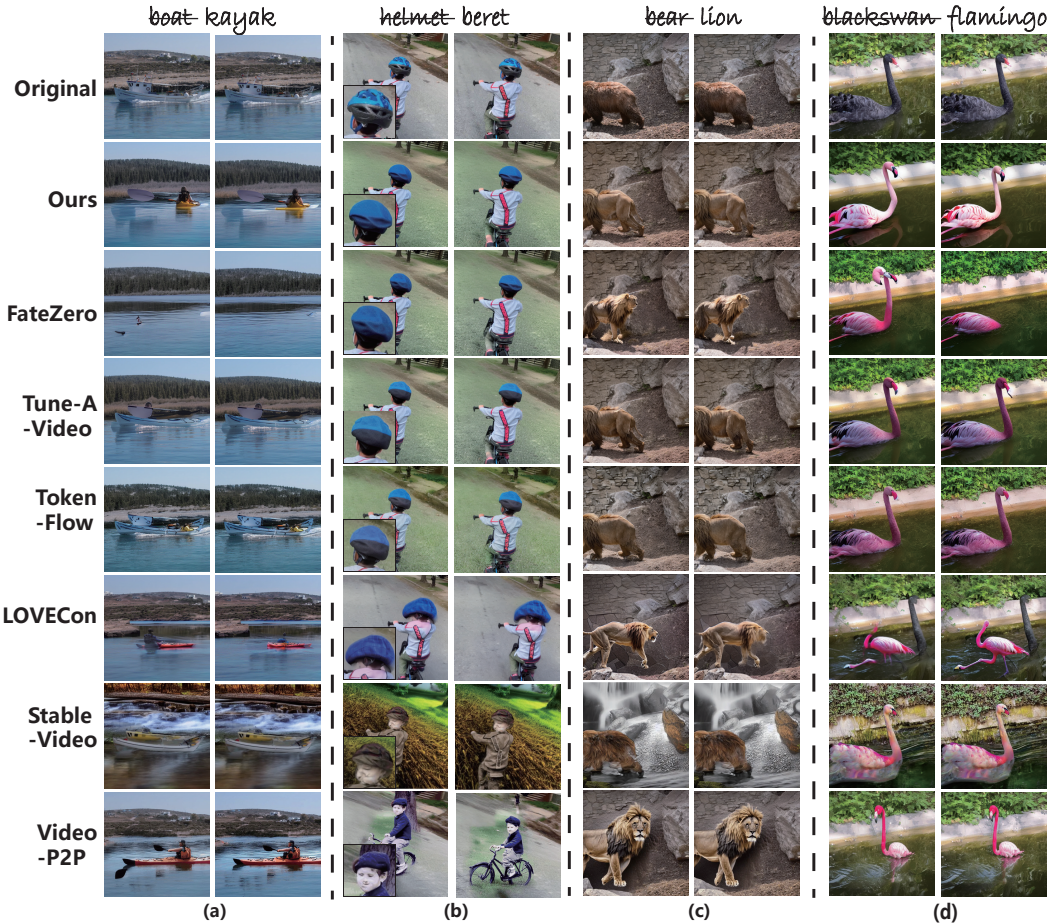


Figure 5: Qualitative comparison with other baselines in shape editing: (a) *boat* → *kayak* and *hill* → *forest*; (b) *helmet* → *beret* and *road* → *grass*, and pose preservation: (c) *bear* → *lion*; (d) *blackswan* → *flamingo*



Figure 6: An example of *RealCraft* applied to a challenging video comprising a fast-moving object and occlusions, spanning 40 frames.

from being overshadowed by existing elements in original frames. Examples can be found in *Fig. 1* and *Fig. 4*. We observe that in our experiments, our approach ensures clean and consistent background transformation.

4.5.3 Precise Shape Editing.

To maintain temporal consistency in video editing, existing methods' edits on objects primarily focus on texture, instead of shape Lee et al. [2023]. As a result of the aforementioned two-step approach, *RealCraft* enables consistent shape editing. As shown in *Fig. 5* (a) and (b), the shape of the original objects is altered to closely match the target's features while maintaining the edits localized and stable across frames.

4.5.4 Pose preservation.

As mentioned by previous research Qi et al. [2023], Wang et al. [2023b], preservation of an object’s pose is crucial to ensure fidelity and temporal consistency. The difficulty increases when the objects described by prompts are not fully visible. For instance, in *Fig. 5 (c)*, despite the bear’s head being left out from the image – a situation that typically complicates editing because distinct features are needed by the prompts to provide enough guidance – *RealCraft* is able to retain the original pose. In *Fig. 5 (d)*, preservation of the original poses and reasonable shape modifications are carried out at the same time, this ability stems from the localized edits made by cross-attention swapping.

4.6 Ablation Study

An ablation study is performed on the 2 types of attention-control components to illustrate of their individual contributions to model performance. As shown in *Fig. 7*, the object white fox is changed to yellow duck and the background transforms from grass to water. With both CROSSBLENDER and SPATIALBLENDER, the vacant areas in the background caused by significant changes are automatically integrated with water. Without CROSSBLENDER, the edits fail to be localized and lead to low editing fidelity. While the absence of SPATIALBLENDER weakens the introduction of the new features, thus resulting in minor change of shape and color. When both are missing, the edited results completely fail to align with the editing prompt’s requirement of “yellow”.

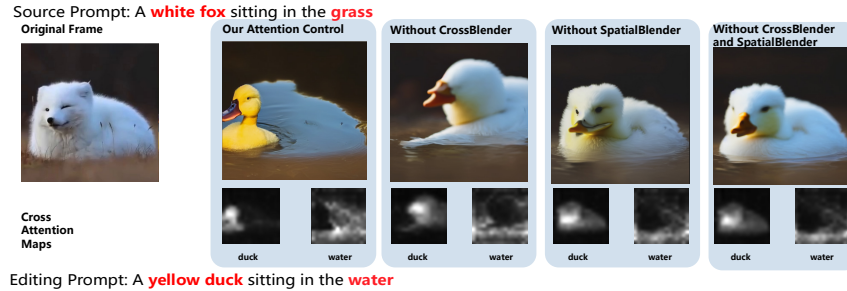


Figure 7: An ablation study on the Attention Control Module’s components for shape editing: The top row displays the original and the generated frames, while the second row illustrates the cross-attention maps for the editing words W^{edit} .

5 Conclusion

In this paper, we introduce *RealCraft*, a parameter-free zero-shot method for editing real videos based on the two key observations we made behind attention mechanisms. Our approach facilitates consistent shape-wise editing across up to 64 frames by simultaneously relaxing spatial-temporal attention and swapping cross-attention. Through quantitative and qualitative evaluation, we demonstrate *RealCraft*’s effectiveness in consistent video editing, background transformation, precise shape editing, and pose preservation. A limitation of the proposed pipeline is its reliance on the performance of Stable Diffusion when extracting the cross-attention maps. Inaccurate maps may lead to sub-optimal edits. One example can be found in supplementary material. This problem can be alleviated by fine-tuning the pre-trained models. Given *RealCraft*’s reliable performance in high-fidelity shape editing with enhanced temporal consistency, future developments could expand the guidance from prompt-only to multi-modal setting, thus expanding the control over object movement (e.g. trajectory, velocity) within scenes and offering users greater creative freedom in their edits.

6 Acknowledgement

This work was partially supported by the Wallenberg AI, Autonomous Systems and Software Program (WASP) funded by the Knut and Alice Wallenberg Foundation. The computations were enabled by the supercomputing resource Berzelius provided by the National Supercomputer Centre at Linköping University and the Knut and Alice Wallenberg Foundation, Sweden.

References

Omer Bar-Tal, Dolev Ofri-Amar, Rafaïl Fridman, Yoni Kasten, and Tali Dekel. Text2live: Text-driven layered image and video editing. In *European conference on computer vision*, pages 707–723. Springer, 2022.

James Betker, Gabriel Goh, Li Jing, Tim Brooks, Jianfeng Wang, Linjie Li, Long Ouyang, Juntang Zhuang, Joyce Lee, Yufei Guo, et al. Improving image generation with better captions, 2023.

Tim Brooks, Bill Peebles, Connor Homes, Will DePue, Yufei Guo, Li Jing, David Schnurr, Joe Taylor, Troy Luhman, Eric Luhman, Clarence Wing Yin Ng, Ricky Wang, and Aditya Ramesh. Video generation models as world simulators. 2024. URL <https://openai.com/research/video-generation-models-as-world-simulators>.

Duygu Ceylan, Chun-Hao P Huang, and Niloy J Mitra. Pix2video: Video editing using image diffusion. In *Proceedings of the IEEE/CVF International Conference on Computer Vision*, pages 23206–23217, 2023.

Wenhao Chai, Xun Guo, Gaoang Wang, and Yan Lu. Stablevideo: Text-driven consistency-aware diffusion video editing. In *Proceedings of the IEEE/CVF International Conference on Computer Vision*, pages 23040–23050, 2023.

Minghao Chen, Iro Laina, and Andrea Vedaldi. Training-free layout control with cross-attention guidance. *arXiv preprint arXiv:2304.03373*, 2023.

Jooyoung Choi, Yunjey Choi, Yunji Kim, Junho Kim, and Sungroh Yoon. Custom-edit: Text-guided image editing with customized diffusion models. *arXiv preprint arXiv:2305.15779*, 2023.

Paul Couairon, Clément Rambour, Jean-Emmanuel Haugéard, and Nicolas Thome. Videdit: Zero-shot and spatially aware text-driven video editing. *arXiv preprint arXiv:2306.08707*, 2023.

Patrick Esser, Johnathan Chiu, Parmida Atighehchian, Jonathan Granskog, and Anastasis Germanidis. Structure and content-guided video synthesis with diffusion models. In *Proceedings of the IEEE/CVF International Conference on Computer Vision*, pages 7346–7356, 2023.

Ruoyu Feng, Wenming Weng, Yanhui Wang, Yuhui Yuan, Jianmin Bao, Chong Luo, Zhibo Chen, and Baining Guo. Credit: Creative and controllable video editing via diffusion models. *arXiv preprint arXiv:2309.16496*, 2023.

Michal Geyer, Omer Bar-Tal, Shai Bagon, and Tali Dekel. Tokenflow: Consistent diffusion features for consistent video editing. *arXiv preprint arXiv:2307.10373*, 2023.

Yutong He, Ruslan Salakhutdinov, and J Zico Kolter. Localized text-to-image generation for free via cross attention control. *arXiv preprint arXiv:2306.14636*, 2023.

Amir Hertz, Ron Mokady, Jay Tenenbaum, Kfir Aberman, Yael Pritch, and Daniel Cohen-Or. Prompt-to-prompt image editing with cross attention control. *arXiv preprint arXiv:2208.01626*, 2022.

Jonathan Ho, Ajay Jain, and Pieter Abbeel. Denoising diffusion probabilistic models. *Advances in neural information processing systems*, 33:6840–6851, 2020.

Jiahui Huang, Leonid Sigal, Kwang Moo Yi, Oliver Wang, and Joon-Young Lee. Inve: Interactive neural video editing. *arXiv preprint arXiv:2307.07663*, 2023.

Hyeonho Jeong and Jong Chul Ye. Ground-a-video: Zero-shot grounded video editing using text-to-image diffusion models. *arXiv preprint arXiv:2310.01107*, 2023.

Yoni Kasten, Dolev Ofri, Oliver Wang, and Tali Dekel. Layered neural atlases for consistent video editing. *ACM Transactions on Graphics (TOG)*, 40(6):1–12, 2021.

Bahjat Kawar, Shiran Zada, Oran Lang, Omer Tov, Huiwen Chang, Tali Dekel, Inbar Mosseri, and Michal Irani. Imagic: Text-based real image editing with diffusion models. In *Proceedings of the IEEE/CVF Conference on Computer Vision and Pattern Recognition*, pages 6007–6017, 2023.

Diederik P Kingma and Max Welling. Auto-encoding variational bayes. *arXiv preprint arXiv:1312.6114*, 2013.

Yao-Chih Lee, Ji-Ze Genevieve Jang, Yi-Ting Chen, Elizabeth Qiu, and Jia-Bin Huang. Shape-aware text-driven layered video editing. In *Proceedings of the IEEE/CVF Conference on Computer Vision and Pattern Recognition*, pages 14317–14326, 2023.

Zhenyi Liao and Zhijie Deng. Lovecon: Text-driven training-free long video editing with controlnet. *arXiv preprint arXiv:2310.09711*, 2023.

Shaoteng Liu, Yuechen Zhang, Wenbo Li, Zhe Lin, and Jiaya Jia. Video-p2p: Video editing with cross-attention control. *arXiv preprint arXiv:2303.04761*, 2023.

Tianyi Lu, Xing Zhang, Jiaxi Gu, Hang Xu, Renjing Pei, Songcen Xu, and Zuxuan Wu. Fuse your latents: Video editing with multi-source latent diffusion models. *arXiv preprint arXiv:2310.16400*, 2023.

Eyal Molad, Eliahu Horwitz, Dani Vavlevski, Alex Rav Acha, Yossi Matias, Yael Pritch, Yaniv Leviathan, and Yedid Hoshen. Dreamix: Video diffusion models are general video editors. *arXiv preprint arXiv:2302.01329*, 2023.

Hao Ouyang, Qiuyu Wang, Yuxi Xiao, Qingyan Bai, Juntao Zhang, Kecheng Zheng, Xiaowei Zhou, Qifeng Chen, and Yujun Shen. Codef: Content deformation fields for temporally consistent video processing. *arXiv preprint arXiv:2308.07926*, 2023.

Geon Yeong Park, Jeongsol Kim, Beomsu Kim, Sang Wan Lee, and Jong Chul Ye. Energy-based cross attention for bayesian context update in text-to-image diffusion models. *arXiv preprint arXiv:2306.09869*, 2023.

Gaurav Parmar, Krishna Kumar Singh, Richard Zhang, Yijun Li, Jingwan Lu, and Jun-Yan Zhu. Zero-shot image-to-image translation. In *ACM SIGGRAPH 2023 Conference Proceedings*, pages 1–11, 2023.

Jordi Pont-Tuset, Federico Perazzi, Sergi Caelles, Pablo Arbeláez, Alex Sorkine-Hornung, and Luc Van Gool. The 2017 davis challenge on video object segmentation. *arXiv preprint arXiv:1704.00675*, 2017.

Chenyang Qi, Xiaodong Cun, Yong Zhang, Chenyang Lei, Xintao Wang, Ying Shan, and Qifeng Chen. Fatezero: Fusing attentions for zero-shot text-based video editing. *arXiv preprint arXiv:2303.09535*, 2023.

Alec Radford, Jong Wook Kim, Chris Hallacy, Aditya Ramesh, Gabriel Goh, Sandhini Agarwal, Girish Sastry, Amanda Askell, Pamela Mishkin, Jack Clark, et al. Learning transferable visual models from natural language supervision. In *International conference on machine learning*, pages 8748–8763. PMLR, 2021.

Robin Rombach, Andreas Blattmann, Dominik Lorenz, Patrick Esser, and Björn Ommer. High-resolution image synthesis with latent diffusion models. In *Proceedings of the IEEE/CVF Conference on Computer Vision and Pattern Recognition (CVPR)*, pages 10684–10695, June 2022a.

Robin Rombach, Andreas Blattmann, Dominik Lorenz, Patrick Esser, and Björn Ommer. High-resolution image synthesis with latent diffusion models. In *Proceedings of the IEEE/CVF conference on computer vision and pattern recognition*, pages 10684–10695, 2022b.

Olaf Ronneberger, Philipp Fischer, and Thomas Brox. U-net: Convolutional networks for biomedical image segmentation. In *Medical Image Computing and Computer-Assisted Intervention–MICCAI 2015: 18th International Conference, Munich, Germany, October 5–9, 2015, Proceedings, Part III* 18, pages 234–241. Springer, 2015.

Chitwan Saharia, William Chan, Saurabh Saxena, Lala Li, Jay Whang, Emily L Denton, Kamyar Ghasemipour, Raphael Gontijo Lopes, Burcu Karagol Ayan, Tim Salimans, et al. Photorealistic text-to-image diffusion models with deep language understanding. *Advances in Neural Information Processing Systems*, 35:36479–36494, 2022.

Shelly Sheynin, Adam Polyak, Uriel Singer, Yuval Kirstain, Amit Zohar, Oron Ashual, Devi Parikh, and Yaniv Taigman. Emu edit: Precise image editing via recognition and generation tasks. *arXiv preprint arXiv:2311.10089*, 2023.

Jiaming Song, Chenlin Meng, and Stefano Ermon. Denoising diffusion implicit models. *arXiv preprint arXiv:2010.02502*, 2020.

Omer Tov, Yuval Alaluf, Yotam Nitzan, Or Patashnik, and Daniel Cohen-Or. Designing an encoder for stylegan image manipulation. *ACM Transactions on Graphics (TOG)*, 40(4):1–14, 2021.

Kai Wang, Fei Yang, Shiqi Yang, Muhammad Atif Butt, and Joost van de Weijer. Dynamic prompt learning: Addressing cross-attention leakage for text-based image editing. *arXiv preprint arXiv:2309.15664*, 2023a.

Wen Wang, Yan Jiang, Kangyang Xie, Zide Liu, Hao Chen, Yue Cao, Xinlong Wang, and Chunhua Shen. Zero-shot video editing using off-the-shelf image diffusion models. *arXiv preprint arXiv:2303.17599*, 2023b.

Jay Zhangjie Wu, Yixiao Ge, Xintao Wang, Stan Weixian Lei, Yuchao Gu, Yufei Shi, Wynne Hsu, Ying Shan, Xiaohu Qie, and Mike Zheng Shou. Tune-a-video: One-shot tuning of image diffusion models for text-to-video generation. In *Proceedings of the IEEE/CVF International Conference on Computer Vision*, pages 7623–7633, 2023.

Hanshu Yan, Jun Hao Liew, Long Mai, Shanchuan Lin, and Jiashi Feng. Magicprop: Diffusion-based video editing via motion-aware appearance propagation. *arXiv preprint arXiv:2309.00908*, 2023.

Shuai Yang, Yifan Zhou, Ziwei Liu, and Chen Change Loy. Rerender a video: Zero-shot text-guided video-to-video translation. *arXiv preprint arXiv:2306.07954*, 2023.

Lvmin Zhang, Anyi Rao, and Maneesh Agrawala. Adding conditional control to text-to-image diffusion models. In *Proceedings of the IEEE/CVF International Conference on Computer Vision*, pages 3836–3847, 2023.

Min Zhao, Rongzhen Wang, Fan Bao, Chongxuan Li, and Jun Zhu. Controlvideo: Adding conditional control for one shot text-to-video editing. *arXiv preprint arXiv:2305.17098*, 2023a.

Yuyang Zhao, Enze Xie, Lanqing Hong, Zhenguo Li, and Gim Hee Lee. Make-a-protagonist: Generic video editing with an ensemble of experts. *arXiv preprint arXiv:2305.08850*, 2023b.